Advances in Science and Technology Research Journal

Advances in Science and Technology Research Journal 2023, 17(4), 271–281
https://doi.org/10.12913/22998624/170713
ISSN 2299-8624, License CC-BY 4.0

Received: 2023.07.05
Accepted: 2023.07.19
Published: 2023.08.15

Numerical and Experimental Investigation of the Effect of Strength of Aluminum 6061 Alloy on Thickness Reduction in Single-Point Incremental Forming

Enas Abdulsada Abbas[1*], Khalida Kadhim Mansor[1]

[1] Department of Production Engineering and Metallurgy, University of Technology, Baghdad, Iraq

* Corresponding author's e-mail: pme.21.65@grad.uotechnology.edu.iq

ABSTRACT

Single-point incremental forming (SPIF) is a kind of incremental sheet forming that is significantly novel. This method involves the utilization of a computer numerical control (CNC) machine to control the path of a forming tool, which is produced by a computer-aided manufacturing program (CAM), as it stretches a metallic sheet to achieve a desired shape. Low patch output and customized parts are good candidates for this kind of technique. The aim of the present investigation is first to study the effect of Aluminum alloy 6061 strength on the thickness distribution and thinning ratio in SPIF and then select the optimal strength to ensure uniform thickness and minimize the thinning. In order to achieve this, two different strengths of Al 6061 sheets have been employed: One used in its original form and the other heat treated to change its strength. Specimens have been prepared using the SPIF procedure for a truncated cone with dimensions of 120 mm diameter and 40 mm depth; the forming slope is 50°, and Solid work program was used to create the tool path. The thickness reduction along the wall portions was analyzed employing the finite element method using Abaqus software, and the numerical results were experimentally confirmed, where the deviation ratio between simulation and experiment was 3% for sample 1 and 5% for sample 2. The findings manifested that the specimens exhibited a consistent distribution of thickness, and the maximum thinning ratio decreased from 30% to 28.5% as the yield strength decreased from 278 MPa to 68.7 MPa, respectively.

Keywords: single-point incremental forming, material strength, thickness distribution, thinning ratio, finite element method

INTRODUCTION

Typically, the metallic sheet component fabrication involves the utilization of specific dies that are manufactured in accordance with the shape and size of the part. This methodology can result in significant delays and costs associated with the production of dies. Due to the ability of large-scale manufacturing to offset the costs associated with the die production, the conventional method is suitable for achieving higher production output. However, there has been a development in flexible die and dieless forming operations for a small-scale production due to the diverse needs of customers, resulting in a reduction in lot size [1]. In today's globally competitive market, one of the most persistent needs of modern industry is to reduce the operational costs and personalize the manufacturing processes. Process of Incremental Sheet Forming (ISF) is a recent, cost-effective technique of sheet metal forming used in rapid prototyping. Its considerable flexibility allows the manufacturers to acquire sheet metal parts with complex, free-form geometries. The ISF technique depicts a great promise in the fields of automotive, aerospace, and medicine [2]. The technique of incremental sheet metal fabrication is a modern and flexible method that includes the manipulation of a metallic sheet using a computer-controlled numerical milling machine. This process involves computer-aided design and manufacturing to manage the tool trajectory, in which

a cylindrical-shaped tool with a hemispherical or spherical-shaped head is used instead of a cutting tool. This tool enables the machine to establish any necessary contour on the sheet without the need for a predetermined die [3]. There are many different incremental forming (IF) technologies that have been developed, including SPIF, Two-Point Incremental Forming (TPIF), and Double-Sided Incremental Forming (DSIF) [4]. Comparing with the other ISF types, SPIF is now the most commonly used incremental forming technique [5], as revealed in Figure 1 [6].

SPIF is a dieless process that can create parts with symmetrical and non-symmetrical geometries and a wide range of thicknesses without the need of expensive dies. It permits the manufacturing of complex sheet metal components at a reasonable cost and is performed on a CNC milling machine that controls the forming tool motion [7]. The sheet is fixed between the backing plates and blank holders, as well as the programmable moving tool with respect to blank holder slides upon the sheet to form the wanted shape [8]. See Figure 2 [9].

In this operation, the distortion is equivalent to the total localized plastic distortions caused by using the tool. The amount of friction produced at the tool and sheet interface can be influenced by table feed, spindle speed, and depth of step, despite the benefits over traditional techniques, including faster prototyping, lower forces, excessively high ability, lower costs, etc. However, there are a few drawbacks to this technique, comprising the slow process, excessively thin material, and lack of dimensional accuracy [10, 11]. One of the key obstacles to the growth of SPIF is the excessive rate of wall thickness thinning. Since the formability of the forming portions is significantly correlated with the thickness thinning ratio, researchers from all over the world have conducted a number of studies on the thickness distribution of formed parts [12]. Li Jun-chao et al. [13] investigated the distribution of thickness as well as mechanical properties of a truncated pyramid manufactured by incremental forming. Following that, the sine law that was employed to estimate the final thickness was confirmed. Furthermore, the relationship among the path of tool, the least thickness, and its location was described. When using a standard tool trajectory, the results evinced that the least thickness is nearly connected with the diameter of tool and depth of step influences

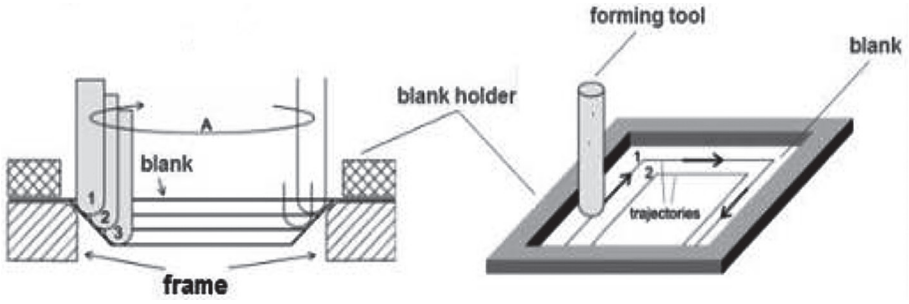

Fig. 1. Representation of the SPIF process [6]

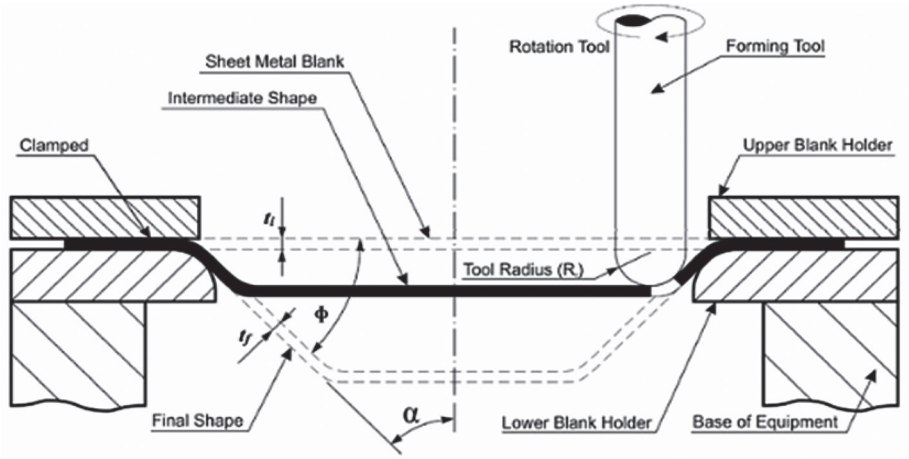

Fig. 2. The schematic representation of the cross-sectional view of rotationally symmetric SPIF method [9]

where it is located significantly. Erika Salem et al. [14] studied the effect of tool strain path upon the AA7075-O sheets formability and localized thinning during the SPIF. As a result of modeling and testing, the measurements evinced that there are three different types of wall portions (bend, thin, and stable). Further, most of the thinning, as predicted by modeling the development of thickness reduction tool, occurred below the tool. Modeling without a damage criterion correctly predicted the thinning of a truncated cone during SPIF. A bending zone with a gradually decreasing thickness was displayed at the beginning of the cone creation. Then, after an initial region of uniform thickness, a much thinner zone formed. Mistuning et al. [15] investigated the thickness thinning, which depends heavily on the shear deformation that happens when a forming tool is used on a sheet of material and for which the sine law is not good enough to predict and control the wall thickness. ABAQUS was used to create the finite element model. The outcomes portrayed that the factors, such as tool diameter, forming angle, and sheet thickness have a considerable impact on the thinning ratio but have a little to no effect on this ratio from the feeding speed. And, the forming angle is the highly robust factor in the thinning ratio, and it can be successfully decreased by employing a forming trajectory with an equally spaced pressing point. Yanle Li et al. [16] focused upon enhancing the mechanical properties (such as yield strength, tensile strength, and hardness), as well as the thickness distribution, by optimization process. Response surface methodology of Box-Behnken design was employed for examining how the various process variables influence the mechanical properties and thickness thinning. Results demonstrated that the larger step down sizes and the larger tools led to a lower maximum thinning rate. The three variables taken into consideration were the tool diameter, step-down size, and sheet thickness. Zeradam Y. et al. [17] studied the thickness distribution of deep drawing quality steel (DDQ) during the SPIF. To predict the thinning in this study, a truncated cone was used. The work used a methodological approach that integrated the numerical modeling, experimental investigation, and theoretical prediction. Results elucidated that the thickness distribution analyzed in the experimental investigation and that anticipated by numerical modeling are in good agreement. The data clearly revealed that the numerical simulation may accurately predict the thinning. Marwan T. Mezher [18] investigated the effects of the diameter of tool as well as forming angle upon the formation of force, the distribution of thickness, ratio of thinning, depth of forming, active plastic strain, and behavior of fracture. Under the same conditions as the experimental inquiry, a model was built utilizing the SPIF of a truncated cone numerical model using the ANSYS program. The results demonstrated that compared to AA1050 aluminum alloy, DC04 carbon steel possesses a higher forming force, a lower least thickness, and a lower ratio of thinning. Sherwan Mohammed Najm et al. [19] explained how the type of coolant, tool speed, feed rates, and diameter of the forming tool affected the hardness of sheet material made of the aluminum alloy AA1100. To calculate the hardness, various regression equations were designed depending upon the search factors. Regression equations allow the scientists to determine the hardness levels reasonably rapidly and practically, as opposed to the experimental method. When the tool speed was increased, the hardness considerably augmented, according to the examination of the test findings. Hardness also rose in correlation with an increase in the feed rate. Furthermore, the impacts of different coolant oils and greases were investigated employing the similar rates of feed; the hardness increased if the coolant oil was utilized, and decreased if the grease was used. Kamel Bensaida et al. [20] analyzed the iterative shaping method that produced a trunk cone using finite element simulation. The effect of geometrical factors (diameter of tool, depth of cut, and path of tool) based on the forming force, distributed stress, and sheet thinning were examined and assessed in this work. The computer modelling of the machining process took into account the impact of tool's trajectory, the vertical step, and the tool's diameter. The results displayed that the thinning of sheet is substantially more relevant in the situation of a continuous tool path (of around 0.2 mm) than it is in the state of a discontinuous tool path.

Many research papers have been published to investigate the effect of SPIF parameters that influence the thinning ratio, with the main goal of these works being to select the best SPIF process parameters to produce parts with a minimum thinning ratio. The researchers' study involved a number of variables, including the diameter of forming tool, shape, size of step, spindle speed, rate of feed, tool path, and others that could have an impact on the thickness distribution and

reduction in thinning. The aim of this research is to find out how the strength of aluminum AA6061 affects the thinning ratio in the SPIF and choose the best strength that gives the lowest thinning ratio, for obtaining a high-quality product made in the SPIF. To achieve this goal, both numerical simulation and experimental work were used. Heat treatment was used to alter the strength of aluminum alloy sheets. The optimal SPIF parameters used to make truncated cones were chosen based on a previous research.

EXPERIMENTAL WORK

Material and process

In this work, two samples of the aluminum alloy AA6061 were used; each sample had a thickness of 1 mm, and it was then cut into dimensions 225 mm x 225 mm. Aluminum AA6061 is a popular alloy because of its acceptable mechanical properties, outstanding weldability, and high corrosion resistance [21].

The chemical composition of aluminum alloy AA6061 was analyzed at the room temperature using the Spector Max equipment, as illustrated in Table 1. The heat-treated AA6061 alloy was designed to have its yield and ultimate strength reduced in this investigation to obtain another case of strength. The annealing heat treatment procedure for this alloy was carried out in an electric furnace at 520 ºC for 10 min, followed by cooling in the furnace [22].

The tensile specimen was prepared according to the ASTM-E8 standard using a water jet as depicted in Figure 3, and the tensile test was conducted using a tensile testing machine model (WDW-200E), to determine the mechanical properties of the materials employed. The load-deflection curve for the two samples of AA6061 alloy is illustrated in Figure 4.

In an effort to make things simpler, the AA6061 alloy at 278 MPa in strength was designated as sample 1, and AA6061 at 68.7 MPa in strength was designated as sample 2. Additionally, Figure 5 reveals the true stress-strain curve for the two samples. Table 2 provides the mechanical characteristics of each sample of AA6061 alloy.

The experimental work was carried out on a C-Tek CNC machine, as viewed in Figure 6, utilizing an oil lubricant, a hemispherical form tool, a (1200 rpm) rotational speed, and a (500 mm/min) travel speed, in accordance with the literature review. A spiral tool pathway was used in this experiment. The dimensions of the part and how the component is displayed in the CNC-part program are explained in Figure 7, which exhibits the shape of the SPIF-made sections as a truncated cone with dimensions (120 mm in diameter, 40 mm in depth, and forming angle).

To theoretically anticipate the thinning estimates, the following formula was used in this research [23]:

$$\varphi = \frac{t - t_0}{t} \cdot 100\% \tag{1}$$

And, the device that used to measure the thickness is an electronic micrometer.

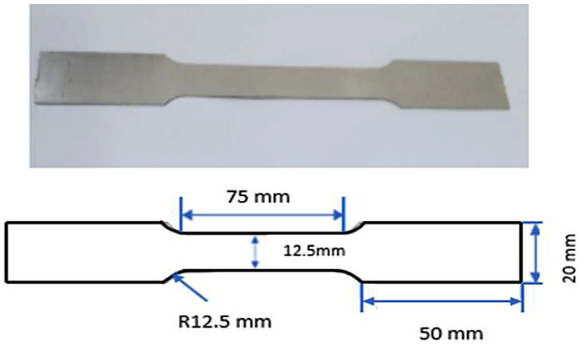

Fig. 3. Standard tensile specimen dimensions

Table 1. The chemical composition of aluminum alloy AA6061

Elements %	Si	Fe	Cu	Mn	Mg	Cr	Ni	Zn	Ti	Pb	Sn	V	Zr	Al
AA6061	0.52	0.389	0.251	0.0392	0.968	0.108	0.0024	0.0010	0.0242	0.0121	0.0005	0.0163	0.0003	97.71

Table 2. The mechanical characteristics of each sample of AA6061 alloy

Material	Ultimate strength, MPa	Yield strength, MPa	Passion ratio	Modulus of elasticity, GPa	Density, kg/m^3
AA6061-Sample 1	365	278	0.33	69	2700
AA6061-Sample 2	147	68.7	0.33	65	2700

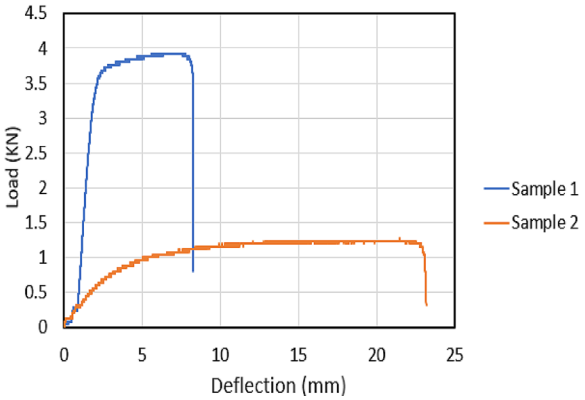

Fig. 4. The load-deflection curve for the two samples of AA6061 alloy

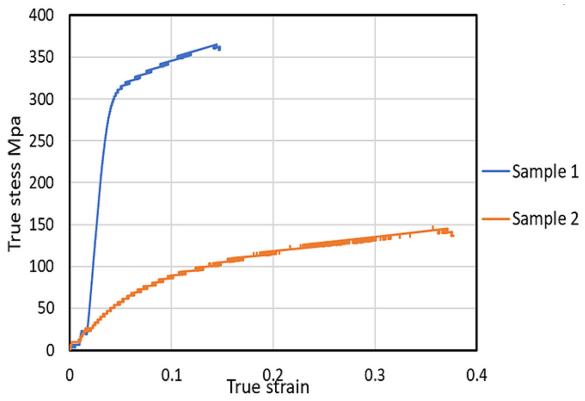

Fig. 5. True stress-strain curve for each sample of AA6061 alloy

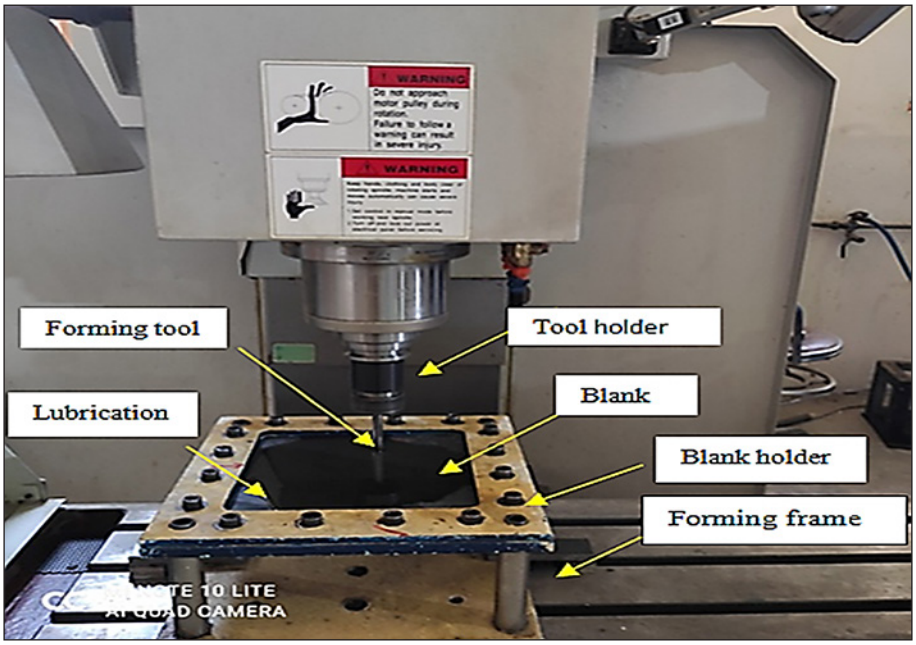

Fig. 6. The used CNC machine

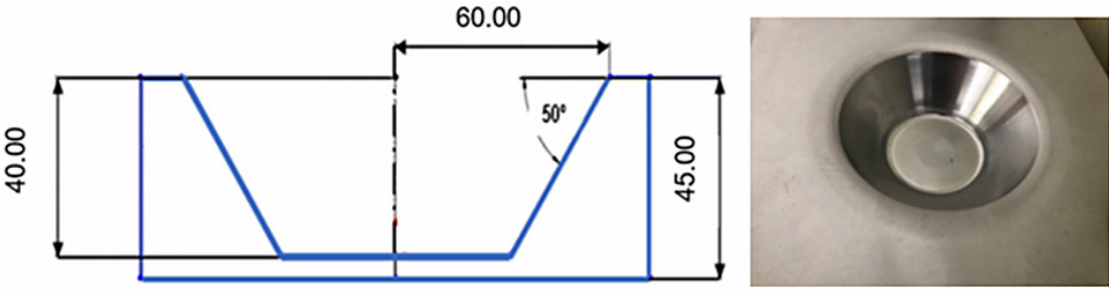

Fig. 7. Part geometry and CNC-part programme. All dimensions are in mm

Finite element simulation

Abaqus/Explicit software was employed in this work to model the SPIF procedure of AA6061 alloy sheets because it can resolve the issues involving geometrically nonlinear difficulties and nonlinear materials. Furthermore, the long contact durations and plastic deformation may be simulated with a high accuracy. According to the research, an explicit resolution approach is the best way to model this process.

The FE model consisted of the following distinct components:

- The tool was modeled as a discrete, rigid body.
- AA6061 sheet was modeled as a deformable body with dimensions 225×225×1 mm.
- Planar shell was in three dimensions.

In contrast, the thickness of sheet was well-defined by the workpiece cross section's features. Between the forming tool and the sheet top surface, a surface-to-surface contact state is established. The sheet is considered to be isotropic, and this study does not investigate the influence of anisotropy. Once the hyperbolic truncated cone attains the depth that has been determined through the experimentation, the FE simulation comes to an end. The SPIF test involves the utilization of a hemispherical tool with a 10 mm diameter, as appeared in Figure 8.

The contact interaction attribute was utilized to specify the communication between the tool and workpiece. Additionally, to model the friction experienced by the AA6061 sheet as it is being formed, a coefficient of 0.1 was selected.

The followings are the boundary conditions that were utilized using the SPIF numerical model:

- The tool was given a rotational velocity about the Z-axis.
- The tool was subjected to linear movement along the X, Y, and Z axes in accordance with the experimental tool path.
- The workpiece was affixed to a fixed support on its four external edges.

The final stage of the truncate cone shape development during the SPIF simulation is displayed in Figure 9. The simulation method was developed to contain a truncate cone shape (120 mm in diameter, 40 mm depth, 0.3 mm step size, 50° forming angle, 1200 m/s feed rate, and 500 rpm rotational speed), as well as a hemispherical forming tool with a diameter of 10 mm.

Utilizing with the view section function, an X-Z section of the component is cut symmetrically; then choosing the "STH" option, which stands for the "sheet thickness". The sheet thickness is then the output for showing the thickness of wall and obtaining the thickness values of 20 points along the section, respectively.

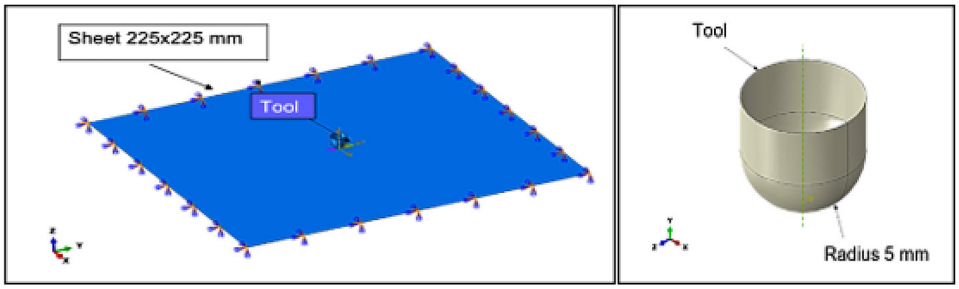

Fig. 8. FE model of the forming tool and sheet

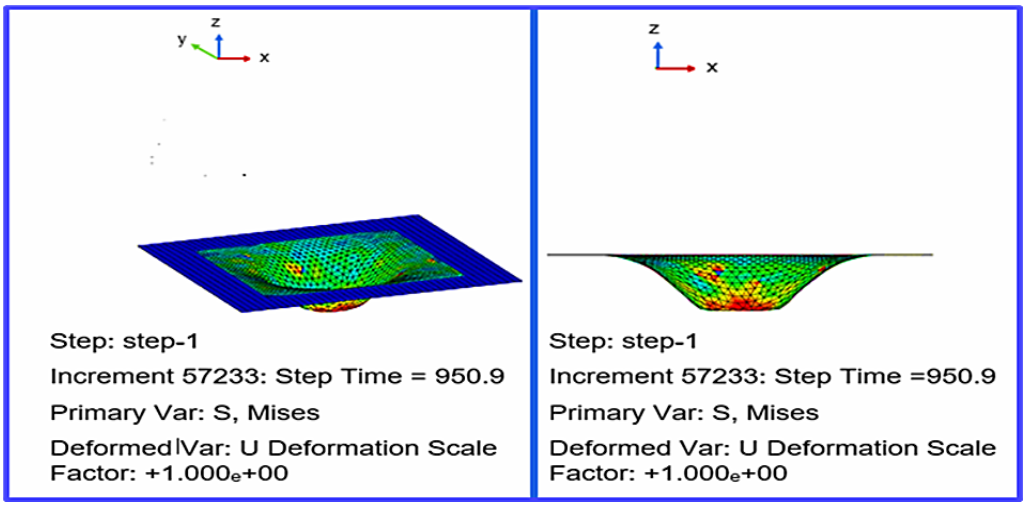

Fig. 9. The final shape in the formation of the truncated cone shape during the SPIF simulation

RESULTS AND DISCUSSION

The reduction in sheet thickness is a crucial parameter in incremental forming techniques, especially in the method of SPIF, as it is closely linked to the formability and potential failure of the resulting products and in the meantime, the portion's wall thinning is significantly impacted by the process parameters. Therefore, this study aims to investigate how the strength of the aluminum 6061 alloy affects the thinning rate and thickness distribution over the length of the shaping component walls during single-point forming using simulated analysis and experimental data. For two cases of AA6061 alloy strength, one at yield strength (278 MPa) and ultimate strength (365 MPa) and the other at yield strength (68 MPa) and ultimate strength (147 MPa) were performed via annealing the heat treatment, as well as the SPIF was performed to execute a symmetric truncated cone having the same geometry.

It is essential to point out that the experiments have been carried out using optimal parameters in order to achieve the least amount of thinning possible, such as a small angle, a small tool diameter, a hemispherical tip shape tool, and a spiral path [7, 11, 14]. It is also important to note that these experiments have been conducted at a safe forming angle of (50º), which is based on the findings of previous studies, and would not lead the product to fail. Consequently, it is significant to make this research concentrate upon the distribution of thickness and the values of thinning at the formed walls.

The components were cut through the thickness of wall, and the values of thickness were obtained by a micrometer having an accuracy of (0.001 mm) while also accounting for the perpendicularity between the part and the micrometer. The points at the zone of deformation alongside the wall's radial direction from the region of clamping to the part's bottom base were chosen for analyzing the behavior of the part. To obtain the average value and reduce the errors for each created portion, the measurements were repeated many times at various locations along the wall, as portrayed in Figure 10.

In reality, there is a fairly intricate thickness distribution alongside the wall, where the thickness is gradually reduces towards the blank holder and continues to decrease until it reaches the maximum thinning at around 30 mm depth near the base.

Measurements, both computational and practical, from the edge that has been clamped to the bottom of the truncated cone, were used to

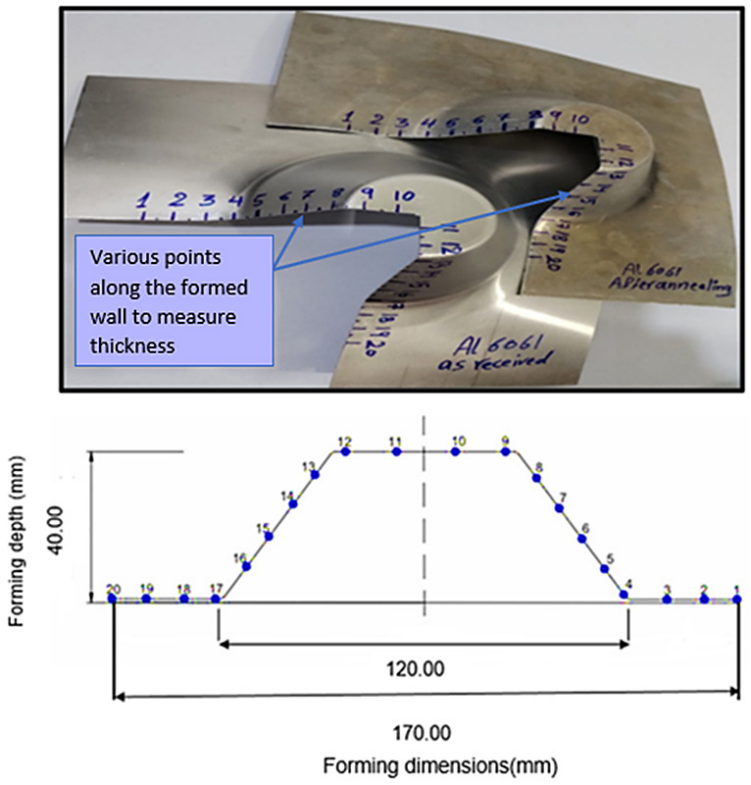

Fig. 10. Various thickness measurement positions along the formed wall of the truncated cone

examine the thickness variations along the wall, as illustrated in figures (11, 12, 13, 14, and 15).

Figures 11 and 12 manifest the simulated and experimental results for the distribution of thickness in the truncated cone wall. In sample 1, the minimum thickness reached 0.730 mm in the simulated result and 0.700 mm in the experimental result, while in sample 2, it reached 0.738 mm and 0.713 mm in the simulated and experimental results, respectively.

Figures 13 and 14 elucidate the numerical results of the thinning ratio in the wall of the truncated cone. In sample 1, the thinning ratio reached 27% in simulated result and 30% in experimental result, while in sample 2, it reached 26% and 28.5% mm in simulated and experimental results respectively. Figure 15 presents the experimental results, which indicate that the maximum thinning ratio reached 30% in sample 1 and 28.5% in sample 2. To simplify the study, the discussion focuses on the experimental results obtained when the thinning ratio values are calculated using equation (1) [15].

It could be noted from the all curves depicted above that the best results in terms of thinning as well as more uniform distribution

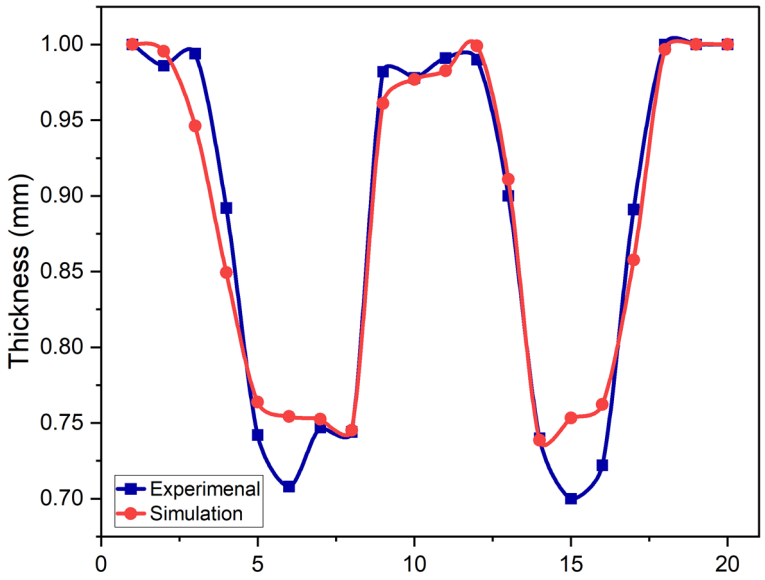

Fig. 11. Simulated and experimental thickness distribution results of AA6061 alloy at yield strength (278 MPa) for sample 1

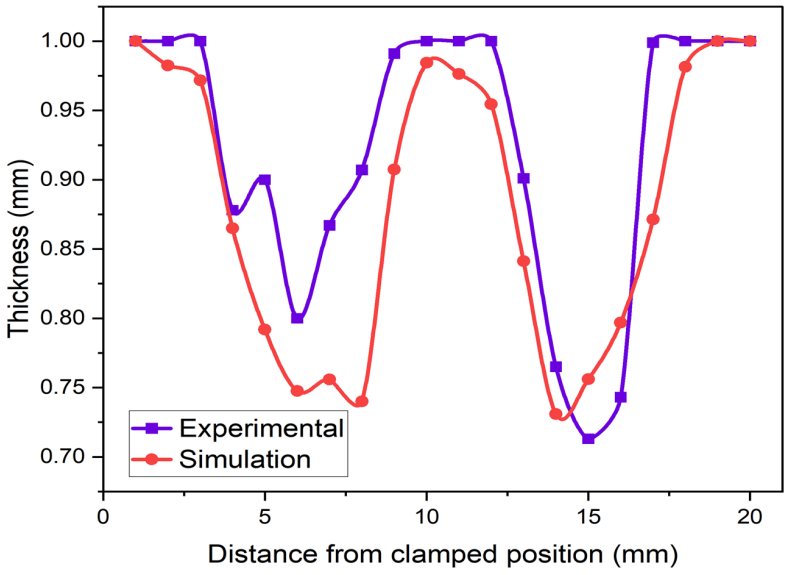

Fig. 12. Simulated and experimental thickness distribution results of AA6061 alloy at yield strength (68.7 MPa) for sample 2

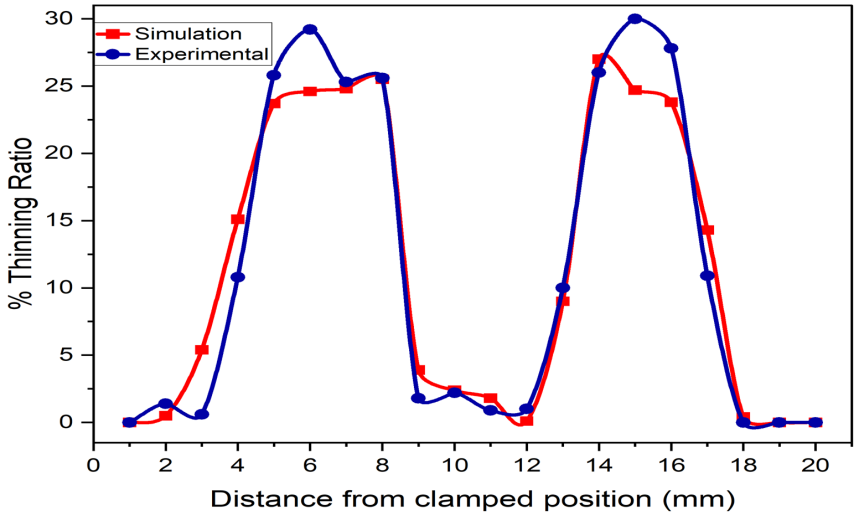

Fig. 13. Simulated and experimental thickness distribution results of AA6061 alloy at yield strength (278 MPa) for sample 1

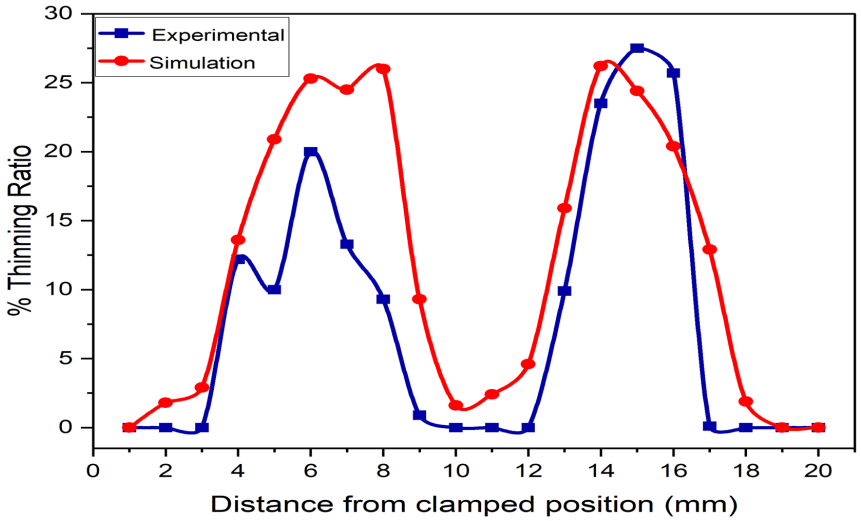

Fig.14. Simulated and experimental thickness distribution results of AA6061 alloy at yield strength (68.7 MPa) for sample 2

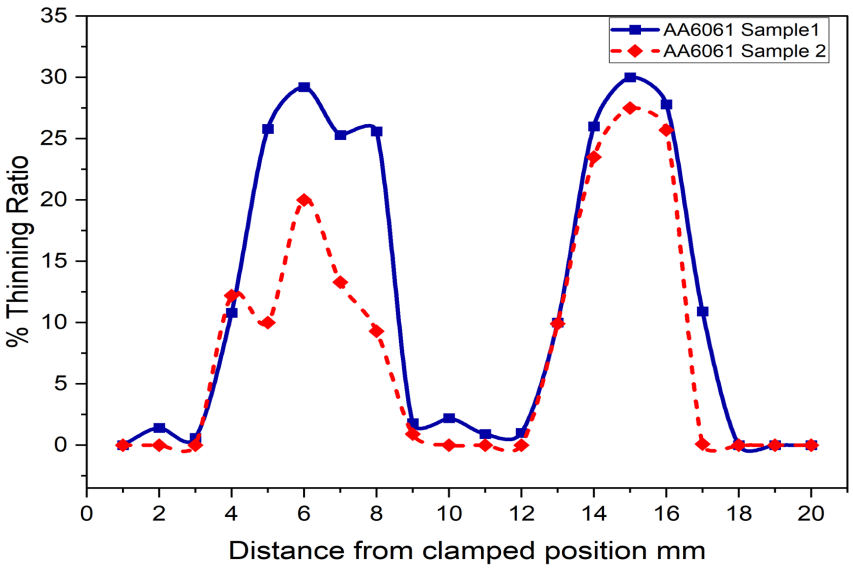

Fig. 15. Chart illustrating the difference between the thinning ratios in the two strength states of AA 6061

of thickness are achieved if the strength drops from 278 MPa to 68.7 MPa and the maximum thinning ratio decreases from 30% to 28.5% as the strength drops. The large thickness reduction along the wall of sample 1 is due to an increase in the amount of plastic deformation that happened in the sheet, which makes the material heavier when it has a high strength compared with sample 2, which has a low strength. That means the material strength has a significant impact on the thinning ratio in the SPIF process compared with the effect of other parameters that impact on the thinning ratio studied by literature review, like tool diameter, step size, and rate of feed which have a little affect [15]. The SPIF is a time-consuming process, and the deformation takes place in the tool-sheet contact region as well as in the deformed wall that is next to the region of contact, causing a localized plastic deformation. The process results in strain hardening of the material, which may lead to the increased strength [23], causing a difficulty in the forming that leads to an irregular thickness distribution; on the other hand, the lower yield strength by heat treatment annealing leads to the increased ductility, which causes a uniform thickness distribution and less thinning. It is important to note that the annealing heat treatment causes a lower strength due to the formation of larger grains, according to reference [21]. It is important to point out that the ratio of variation between the simulation and the experiment is 2% for sample 1 and 5% for sample 2, respectively. The numerical results, on the other hand, were affected by a variety of simplifications such as the assumptions that the tool is a rigid body, there is no temperature, there are no heat transfers, and the friction that exists between the tool and the sheet is always the same during the process of forming. Nevertheless, they were predicted with an important degree of accuracy despite the fact that the thickness measured in the experiments was higher than that of the numerical values with respect to the maximum thinning ratio, which reached 27% in sample 1, while in the experiment, it was 30%, and in sample 2, the maximum thinning ratio reached 26%, while in the experiment, it was 28.5%.

These findings indicate a direct proportionality between the thinning ratio and yield strength, such that a reduction in the yield strength causes a reduction in the thinning ratio

CONCLUSIONS

Thickness thinning is a crucial aspect of the SPIF process since it establishes the sheet's limitations for forming, while the process variables have an impact on the measured thickness as well as thinning, and, consequently, the finished product quality. Experimental measurements were taken to determine the deviation in thickness and the reduction ratio of the formed portions along an inclining wall of the finished product of the two sheets of AA6061 alloy using the SPIF procedure, with the aim of achieving the best result with regard to the minimum thinning.

In this study a comprehensive analysis was conducted, both numerical and experimental, to examine the correlation between the AA6061 alloy strength and the distribution of thickness along the wall, so the obtained results include:

1. The thickness distribution is greatly influenced by the material's strength. According to both experimental and numerical findings, which demonstrated that the maximum thinning decreased from 30% at a strength value of 278 MPa to 28.5% at a strength value of 68.7 MPa, the thickness distribution uniformity alongside the profile of the wall has been observed for AA6061 alloy sheet with lower strength.
2. In the experiment, the settings of forming were chosen using a thin metallic sheet, a smaller forming angle, a smaller diameter and hemispherical tool head, and a smaller step down to achieve a lower thinning ratio, according to the literature, to increase the forming precision.
3. The yield strength of AA6061 reduced from 278 MPa to 68.7 MPa by annealing heat treatment, this reduction in yield strength can be attributed to the formation of larger grains and resulted in reducing the thinning ratio.
4. The maximum thinning ratio determined from the simulation and experiment is 27% and 30% for sample 1 and 26% and 28.5% for sample 2, respectively, revealing the accuracy and dependability of the simulation's findings. There is some difference between the simulation and experiment outcomes, but it's noticeably small, where the deviation ratio is 2% at sample 1 and 5% at sample 2. This is due to the fact that the forming tool is considered to be a rigid body in the procedure of modeling, and the friction that exists between the sheet and the tool is always constant. As a result, the thickness distribution and thinning ratios can be predicted with a reasonable accuracy using a computer simulation.

REFERENCES

1. Abbas, T.F., Younis, K.M., Kadhim, M.K., The influence of process parameters on thickness distribution in multipoint forming process using finite element analysis. In: 2019 2nd International Conference on Electrical, Communication, Computer, Power and Control Engineering (ICECCPCE), 2019: 120-125.
2. Mulay, A., Hirani, H., Choudhary, S.K., Numerical modeling and optimization with novel process parameters in the incremental forming of DC04 sheets. Journal of Materials Engineering and Performance, 32(5), 2023: 2344-2355.
3. Hamdan, W.K., Mohamed, J.H., Obaeed, N.H., Influence of some relevant process parameters on the surface roughness of surfaces produced by ISMF process. Engineering and Technology Journal, 32(8 Part (A), 2014.
4. Wang, Y., Wang, L., Zhang, H., Gu, Y., Ye, Y., A novel algorithm for thickness prediction in incremental sheet metal forming. Materials, 15(3), 2022: 1201.
5. Krasowski, B., Kubit, A., Trzepieciński, T., Dudek, K., Slota, J, Application of X-ray diffraction for residual stress analysis in truncated cones made by incremental forming. Advances in Science and Technology. Research Journal, 14(2), 2020.
6. Bedan, A.S., and Habeeb, H.A., Experimental study the effect of tool geometry on dimensional accuracy in single point incremental forming (SPIF) process. Al-Nahrain Journal for Engineering Sciences, 21(1), 2018: 108-117.
7. Jabar, M.A., and Younis, M.K., Effects of process parameters in incremental sheet metal forming using visioplasticity method. Engineering and Technology Journal, 34(12), 2016: 2334-2346.
8. Bhasker, R.S., and Kumar, Y., Process capabilities and future scope of incremental sheet forming (ISF). Materials Today: Proceedings, 72, 2023: 1014-1019.
9. Gatea, S., Ou, H., McCartney, G., Review on the influence of process parameters in incremental sheet forming. The International Journal of Advanced Manufacturing Technology, 87, 2016: 479-499.
10. Mulay, A., Ben, B.S., Ismail, S., Kocanda, A., Jasiński, C., Performance evaluation of high-speed incremental sheet forming technology for AA5754 H22 aluminum and DC04 steel sheets. Archives of Civil and Mechanical Engineering, 18, 2018: 1275-1287.
11. Bedan, A.S., Algodi, S.J., Hussain, E.A., Investigating the effect of hybrid process: MPF/SPIF on the microstructure and mechanical properties of brass (65-35) sheet. Advances in Science and Technology. Research Journal, 17(3), 2023: 302-308.
12. Khudhir W.S., Jaber A.Sh., Shukur J.J., Analysis of the process parameters effect on the thickness distribution and thinning ratio in single point incremental forming process. Journal of Mechanical Engineering Research and Developments, 43(7), 2020: 374-382.
13. Li Junchao, L.I. Chong, Tong-gui Zhou, Thickness distribution and mechanical property of sheet metal incremental forming based on numerical simulation. Transactions of Nonferrous Metals Society of China, 22, 2012: 54-60.
14. Salem E., et al., Investigation of thickness variation in single point incremental forming. Procedia Manufacturing, 5, 2016: 828-837.
15. Yang Mingshun, et al., Study on thickness thinning ratio of the forming parts in single point incremental forming process. Advances in Materials Science and Engineering, 2018.
16. Li Yanle, et al., Effects of process parameters on thickness thinning and mechanical properties of the formed parts in incremental sheet forming. The International Journal of Advanced Manufacturing Technology, 98(9), 2018: 3071-3080.
17. Zeradam, Y. and Krishnaiah, A., Numerical simulation and experimental validation of thickness distribution in single point incremental forming for drawing quality steel. Int. J. Appl. Eng. Res, 15(1), 2020: 101-107.
18. Mezher M.T., and Kovács B., An investigation of the impact of forming process parameters in single point incremental forming using experimental and numerical verification. Periodica Polytechnica Mechanical Engineering, 2022.
19. Najm Sherwan M., et al., Parametric effects of single point incremental forming on hardness of AA1100 aluminium alloy sheets. Materials, 14(23), 2021: 7263.
20. Bensaid, K., Souissi, R., Boulila, A., Ayadi, M., Ben Fredj, N., Numerical investigation of incremental forming process of AISI 304 stainless steel. Ironmaking & Steelmaking, 50(2), 2023: 174-183.
21. Darzi, S., Mirnia, M.J., Elyasi, M., Single-point incremental forming of AA6061 aluminum alloy at elevated temperatures. The International Journal of Advanced Manufacturing Technology. 116(3-4), 2021: 1023-1039.
22. Mohammadi, M., and Ashtiani, H.R., Influence of heat treatment on the AA6061 and AA6063 aluminum alloys behavior at elevated deformation temperature. Iranian Journal of Materials Science & Engineering, 18(2), 2021.
23. Kumar, G., and Maji, K., Investigations into enhanced formability of AA5083 aluminum alloy sheet in single-point incremental forming. Journal of Materials Engineering and Performance, 30, 2021: 1289-1305.